New phase space calculations for β-decay half-lives

Sabin Stoica[1,2], Mihail Mirea[1,2], Ovidiu Niţescu[2,3]
[1] *Horia Hulubei Foundation, P.O. MG6, 077125-Magurele, Romania,*
[2] *Horia Hulubei National Institute of Physics and Nuclear Engineering, P.O. Box MG6, 077125-Magurele, Romania,*
[3] *University of Bucharest, Faculty of Physics, P.O. Box MG11, 077125-Magurele, Romania**

Jameel-Un Nabi
GIK Institute of Engineering Sciences and Technology, Topi 23640, Khyber Pakhtunkhwa, Pakistan.

Mavra Ishfaq
GIK Institute of Engineering Sciences and Technology, Topi 23640, Khyber Pakhtunkhwa, Pakistan.

(Dated: July 18, 2016)

We revisit the computation of the phase space factors (PSF) involved in the positron decay and electron capture (EC) processes for a large number of nuclei of experimental interest. To obtain the electron/positron wave functions needed in computation, we develop a code for solving accurately the Dirac equation with a nuclear potential derived from a realistic proton density distribution in the nucleus. The finite nuclear size (FNS) and screening effects are included through recipes which differ from those used in previous calculations. Comparing our results with former calculations employing approximate methods but computed with the same Q-values, we find a close agreement for positron decays, while for the EC process there are relevant differences. For the EC process we also find that the screening effect has a notable influence on the computed PSF values specially for light nuclei. Further, we re-computed the same PSF values but using the most recent Q-values reported in literature. In several cases these new Q-values differ significantly from the older ones, which results in large differences in the PSF values as compared with previous results. These new PSF values proposed here, can contribute to a more reliable calculation of the beta decay rates, which are key quantities in the study of nuclei far from the stability line, as well as to better understanding of the stellar evolution.

PACS numbers: 23.40.Bw; 23.40.-s; 26.30.Jk

arXiv:1607.04426v1 [nucl-th] 15 Jul 2016

I. INTRODUCTION

The phase space factors for beta decay and electron capture were calculated since long time [1–3] and were considered to be evaluated with sufficient accuracy. However, in those works the distortion of the electron wave functions (w.f.) by the Coulomb field of the nucleus was taken into account through Fermi functions which were expressed in terms of approximate radial solutions of the Dirac equation at the nuclear surface. Also, other corrections were introduced in the calculations in approximate ways. Thus, the screening effect on the β spectrum was included by various recipes, for example by replacing the V(Z) potential with a momentum dependent screening (for low energy positrons) [3], by modifying the electron radial w.f. [4]-[5], etc. Also, the finite size of the nucleus (FNS) was taken into account by adding to the Fermi functions obtained in the "point-nucleus" approximation, corrections that depend on the β particle energy and nuclear charge Z [6, 7]. Also, for the nuclear radius, older formula has been used [3, 8]. For the EC process the electron bound-state radial w.f. were also obtained as approximate solution of the Dirac equation evaluated at the nuclear surface. They were improved by including exchange and overlap corrections, which were obtained within a relativistic HF approach.

In this work we revisit the computation of the PSF involved in the positron decay and electron capture (EC) processes for light and heavy nuclei of experimental interest. The Dirac equation is solved numerically with a Coulomb potential derived from a realistic proton distribution in the nucleus which includes the FNS correction. The numerical procedure follows the power series method described in Ref. [9] and is similar to that described in Refs. [10, 11]. The screening effect was introduced by using a screened Coulomb potential, obtained by multiplying the Coulomb potential by a function $\phi(x)$, solution of the Thomas-Fermi equation obtained by the Majorana method [12]. The accuracy imposed in our numerical algorithms used to solve the Dirac equation always exceeds the convergence criteria given in those references. Also, a more efficient procedure to identify the electron bound states without ambiguity was developed.

In order to make a comparison between the actual PSF values found in literature and ours, the same PSF are also computed with the approach described in Refs. [2, 3] and using the same Q-values. For positron decays our results are in close agreement with the other previous results, while for the EC process we found significant differences. For these processes we also find that the screening ef-

* stoica@theory.nipne.ro; Also at Horia Hulubei Foundation, P.O. MG12, 077125-Magurele, Romania.

fect has a notable influence on the computed PSF values for light nuclei. Further, we re-computed the same PSF values using up-dated Q values, reported recently in literature [13], which for several light nuclei differ significantly from the older ones. As an example we cite the maximum β-particle energy (referred to as W_0 throughout this paper) stated in Table 2 of Ref. [14]. These W_0 values differ considerably from those given in Ref. [13]. One reason for this big difference could be that Wilkinson & Macefield, in order to compare their calculation with those performed earlier by Towner & Hardy [15], restricted their phase space to only pure Fermi transitions. In other words the Gamow-Teller window was not accessed in phase space calculation of [14]. Thus, in this paper we propose new PSF values computed with a more accurate method and using up-dated Q-values, for a large number of nuclei of experimental interest. Our calculations can be useful for more reliable computation of the beta decay rates of nuclei far from the stability line, as well as for better understanding of the stellar evolution.

Our work is further motivated by similar calculations done for the double-beta decay (DBD) process. The PSF for DBD were also considered for a long time to be computed with enough accuracy and were used as such for predicting DBD lifetimes. However, recently, they were recalculated with improved methods, especially for positron and EC decay modes [16, 18] and several differences were found as compared to previous calculations where approximate electron/positron w.f. were used.

The paper is organized as follows. In Section II we present briefly the two approaches used to compute our PSF values. Our results are reported in Section III. Here we compare them with experimental data and previous results and discuss the differences. Finally, we summarize the main points and present our conclusions in Section IV.

II. FORMALISM

Following essentially the formalism from Ref. [3], we give here the necessary equations which we use to calculate the PSF.

A. Phase space factors for β^+ transitions

The probability per unit time that a nucleus with atomic mass A and charge Z decays for an allowed β-branch is given by:

$$\lambda_0 = g^2/2\pi^3 \int_1^{W_0} pW(W_0 - W)^2 S_0(Z,W) dW, \quad (1)$$

where g is the weak interaction coupling constant, p is the momentum of β-particle, $W = \sqrt{p^2+1}$ is the total energy of β-particle and W_0 is the maximum β-particle energy. $W_0 = Q-1$, in β^+decay (Q is the mass difference between initial and final states of neutral atoms). Eq. (1) is written in natural units ($\hbar = m = c = 1$) so that the unit of momentum is mc, the unit of energy is mc^2, and the unit of time is $\hbar\ /mc^2$. The shape factors $S_0(Z,W)$ for allowed transitions which appear in Eq. (1) are defined as:

$$S_0(Z,W) = \lambda_1(Z,W)|M_{0,1}|^2, \quad (2)$$

where $M_{0,1}$ are the nuclear matrix elements and the Fermi functions $\lambda_1(Z,W)$. Thus, for calculating the β^+ decay rates one needs to calculate the nuclear matrix elements and the PSF, that can be defined as:

$$F_{BP} = \int_1^{W_0} pW(W_0 - W)^2 \lambda_1(W) dW. \quad (3)$$

For the allowed β decays the Fermi functions are expressed as:

$$\lambda_1(Z,W) = \frac{g_{-1}^2 + f_1^2}{2p^2}, \quad (4)$$

where $g_{-1}(Z,W)$ and $f_1(Z,W)$ are the large and the small radial components of the positron radial wave functions evaluated at the nuclear radius R which can be obtained by solving the Dirac equation:

$$\left(\frac{d}{dr} + \frac{\kappa}{r}\right) g_\kappa(W,r) = (W + V + 1) f_\kappa(W,r) \quad (5)$$
$$\left(\frac{d}{dr} + \frac{\kappa}{r}\right) f_\kappa(W,r) = -(W + V - 1) g_\kappa(W,r)$$

where V is the central potential for the positron and $\kappa = (l-j)(2j+1)$ is the relativistic quantum number. We note that Eq. (5) is also written in natural units.

An important step in the PSF calculation for β^+ decay is the method of obtaining the positron continuum radial functions. For this we develop a new method (code) of solving the Dirac equation, which is adapted from the method used previously for the computation of PSF for DBD process [17, 18].

We solved Eq. (5) in a nuclear potential $V(r)$ derived from a realistic proton density distribution in the nucleus. This is done by solving the Schrodinger equation with a Woods-Saxon potential. In this case:

$$V(Z,r) = \alpha\hbar c \int \frac{\rho_e(\vec{r'})}{\mid \vec{r} - \vec{r'} \mid} d\vec{r'}, \quad (6)$$

where the charge density is

$$\rho_e(\vec{r}) = \sum_i (2j_i + 1) v_i^2 \mid \Psi_i(\vec{r}) \mid^2, \quad (7)$$

Ψ_i is the proton (Woods-Saxon) w.f. of the spherical single particle state i and v_i is its occupation amplitude. The factor $(2j_i + 1)$ reflects the spin degeneracy.

The screening effect is taken into account by multiplying the expression of $V(r)$ with a function $\phi(r)$, which is the solution of the Thomas Fermi equation: $d^2\phi/dx^2 = \phi^{3/2}/\sqrt{x}$, with $x = r/b$, $b \approx 0.8853 a_0 Z^{-1/3}$ and a_0 = Bohr radius. It is calculated within the Majorana method [12]. The boundary conditions are $\phi(0) = 1$ and $\phi(\infty) = 0$. As mentioned above the screening effect is taken into account by a method developed in Ref. [12]. The possible ways in which the screening function modifies the Coulomb potential depends on the specific mechanism and its boundary conditions.

For the case of the β^+-decay process, the potential used to obtain the electron w.f. is

$$rV_{\beta^+}(Z,r) = (rV(Z,r) + 1) \times \phi(r) - 1 \tag{8}$$

to take into account the fact that β decay releases a final negative ion with charge -1. $V(Z,r)$ is positive. In our approach, we considered the solution of the Thomas-Fermi equation as a universal function, giving an effective screening. Here, the product $\alpha\hbar c = 1$, for atomic units. The asymptotic potential between an positron and an ionized atom is $rV_{\beta^+} = -1$. In this case, the charge number $Z = Z_0 - 1$ corresponds to the daughter nucleus, Z_0 being the charge number of the parent nucleus. Asymptotically $\phi(r)$ tends to zero.

In this case the radial solutions of the Dirac equations should be normalized in order to have the following asymptotic behavior

$$\begin{pmatrix} g_k(\epsilon,r) \\ f_k(\epsilon,r) \end{pmatrix} \sim \frac{\hbar e^{-i\delta_k}}{pr} \begin{pmatrix} \sqrt{\frac{\epsilon+m_ec^2}{2\epsilon}}\sin(kr - l\frac{\pi}{2} - \eta\ln(2kr) + \delta_k) \\ \sqrt{\frac{\epsilon-m_ec^2}{2\epsilon}}\cos(kr - l\frac{\pi}{2} - \eta\ln(2kr) + \delta_k) \end{pmatrix}, \tag{9}$$

where c is the speed of the light, m_e/ϵ are the electron mass/energy, $k = p/\hbar$ is the electron wave number, $\eta = Ze^2/\hbar v$ (with $Z = \pm Z$ for $\beta^\mp$ decays), is the Sommerfeld parameter, δ_κ is the phase shift and V is the Coulomb interaction energy between the electron and the daughter nucleus.

On the other side we also calculated the PSF for positron decays with the method described in [3]. The g_k and f_k functions were calculated by solving the Dirac equation for a point-nucleus unscreened Coulomb potential, for which the equation has analytical solutions. The finite nuclear size and screening effects were introduced as corrections, after the recipe described in [3]. The finite size correction was introduced by means of an empirical deviation that depended on the atomic mass Z and the energy W [6, 7]. The screening correction was given by the following replacement [4, 5]:

$$g^2_{-1}(Z,W) \to \frac{pW'}{p'W} g^2_{-1}(Z,W')$$

$$f^2_{-1}(Z,W) \to \frac{pW'}{p'W} f^2_1(Z,W'), \tag{10}$$

where $W' = W + V_0$, $p' = \sqrt{(W')^2 - 1}$ and V_0 was taken as a p-dependent screening potential. For further details of this formalism we refer to [3]. No electromagnetic corrections were undertaken in this calculation of PSF.

B. Phase space factors for electron capture (EC)

Electron capture is always an alternate decay mode for radioactive isotopes that do not have sufficient energy to decay by positron emission. This is a process which competes with positron decay. In order for electron capture leading to a vacancy in, say, the K-shell, the atomic mass difference between initial and final states, Q, must be greater than the binding energy of a K-shell electron in the daughter atom, ϵ_K. The energy carried off by the neutrino is then given by

$$q_K = Q - \epsilon_K \tag{11}$$

If the energy requirement $Q > \epsilon_K$ is satisfied, electron capture from the K-shell is more probable than that from any other shell because of the greater density at the nucleus of the K-shell electrons. The total K-shell capture rate can be expressed as

$$\lambda^0_{EC,K} = \lambda^0_K B_K, \tag{12}$$

where

$$\lambda^0_K = \frac{g^2|M_{0,1}|^2}{4\pi^2} q^2_K g^2_K, \tag{13}$$

where g^2 is a constant (with dimensions of t^{-1}), the M's are specific combinations of nuclear matrix elements, g_K is the large component of the bound-state radial w.f. of the captured K-shell electron (evaluated at the nuclear surface R_A), q_K is the neutrino energy in units of mc^2 and B_K is the "exchange" correction factor for the K-shell. In analogy with Eq. (12), the L-shell total capture rate will be

$$\lambda^0_{EC,L_i} = \lambda^0_{L_i} B_{L_i}, \tag{14}$$

where L_i denotes a particular L-subshell. The contribution of L_1 pertaining to the $2s_{1/2}$ orbital is the most important, so we keep in our calculations only the contribution of this subshell to the calculated our PSF. The expressions for $\lambda^0_{L_1}$ can be obtained from Eq. (13) by

the replacement of q_K, g_K by q_{L_1}, g_{L_1}. Electron capture from the M-, N- and higher shells may be defined in a similar fashion, but they have negligible contributions in comparison with the K- and L- ones.

Hence, for an allowed transition, the PSF expression of electron capture within the approximation stated above, can be written as

$$F_{EC}^{K,L_1} = \frac{\pi}{2}\left(q_K^2 g_K^2 B_K + q_{L_1}^2 g_{L_1}^2 B_{L_1}\right). \tag{15}$$

For the q_{K/L_1} quantities we used the expression

$$q_{K/L_1} = W_{EC} - \epsilon_{K/L_1}, \tag{16}$$

were, W_{EC} is the Q value of the β^+ decay in $m_e c^2$ units, ϵ_i are the binding energies of the $1s_{1/2}$ and $2s_{1/2}$ electron orbitals of the parent nucleus, g_i their radial densities on the nuclear surface. $B_i \approx 1$ represent the values of the exchange correction. These are due to an imperfect overlap of the initial and final atomic states caused by the one unit charge difference [19]. In our method we consider these exchange corrections to be unity, for the nuclei considered, the estimated error in doing that being under 1%. The relation $W_0 = W_{EC} - 1$ holds.

The g_{K/L_1} are the electron bound states, solutions of the Dirac equation (5), and correspond to the eigenvalues ϵ_n (n is the radial quantum number). The quantum number κ is related to the total angular momentum $j_\kappa = \mid \kappa \mid -1/2$. These w.f. are normalized such that

$$\int_0^\infty [g_{n,\kappa}^2(r) + f_{n,\kappa}^2(r)]dr = 1. \tag{17}$$

For simplicity, we consider solutions of the Dirac equations $g_{n,\kappa}$ and $f_{n,\kappa}$ that are divided by the radial distance r. An asymptotic solution is obtained by means of the WKB approximation and by considering that the potential V is negligible small:

$$\frac{f_{n,\kappa}}{g_{n,\kappa}} = \frac{c\hbar}{\epsilon + m_e c^2}\left(\frac{g'_{n,\kappa}}{g_{n,\kappa}} + \frac{\kappa}{r}\right), \tag{18}$$

where

$$\frac{g'_{n,\kappa}}{g_{n,\kappa}} = -\frac{1}{2}\mu'\mu^{-1} - \mu, \tag{19}$$

with

$$\mu = \left[\frac{\epsilon + m_e c^2}{\hbar^2 c^2}(V - \epsilon + m_e c^2) + \frac{\kappa^2}{r^2}\right]^{1/2}. \tag{20}$$

In our calculations we use the number node n=0 and n=1, for the orbitals $1s_{1/2}$ and $2s_{1/2}$, respectively, κ being -1. Numerically, the eigenvalues of the discrete spectrum are obtained by matching two numerical solutions of the Dirac equation: the inverse solution that starts from the asymptotic conditions and the direct one that starts at r=0.

The radial density of the bound state electron w.f. on the nuclear surface is:

$$D_{n,\kappa}^2 = \frac{1}{(m_e c^2)^3}\left(\frac{\hbar c}{a_0}\right)^3\left(\frac{a_0}{R_A}\right)^2\left[g_{n,\kappa}^2(R_A) + f_{n,\kappa}^2(R_A)\right], \tag{21}$$

where $R_A = 1.2A_0^{1/3}$ is given in fm, a_0 being the Bohr radius. For the $1s_{1/2}$ and $2s_{1/2}$ electron orbitals, we use $g_K^2 = D_{0,-1}^2$ and $g_{L_1}^2 = D_{1,-1}^2$, respectively.

For the EC processes, the potential used to obtain the electron w.f. reads

$$rV_{EC}(Z,r) = rV(Z,r)\phi(r), \tag{22}$$

and the charge number $Z = Z_0$ corresponds to the parent nucleus. $V(Z,r)$ is negative.

The numerical solutions of the Dirac equation were obtained within the power series method of Ref. [9], by using similar numerical algorithm as that of Refs. [10, 11]. The method is able to provide numerical solutions of the Dirac equation for central fields. We provide a grid with values of the potential for different radial distances. The radial w.f. is expanded in an infinite power series that depends on the radial increment and the potential values. The w.f. is calculated step by step in the mesh points. The increment and the number of terms in the series expansion determine the accuracy of the solutions. In our calculations, the increment interval is 10^{-4} fm and at lest 100 terms are taken into account in the series expansion. These values exceed the convergence criteria of Ref. [10]. To renormalize the numerical solutions, we made use of the fact that at very large distances, the behavior of the w.f. must approach that of the Coulomb function. Therefore, the the amplitudes and the the phase shifts can be extracted by comparing the numerical solution and the analytical ones. For discrete states, the asymptotic behavior of the w.f. gives a guess for the inverse solutions. The eigenvalue is obtained when the direct solutions and the inverse ones match each other. We constructed an adequate procedure to find the bound states of the electron up to an accuracy of 0.3 keV, or lower, by searching solutions up to 130 keV binding energies. In this range of energies, all the possible bound state energies are found. We calculated the solutions starting outward from $r = 0$ and inward from a very large value of the radius r. The bound states should be obtained when both solutions are equal in an intermediate point, for the two components of the wave function. We found these energies by interpolation. We selected the radial wave functions $f_{n,\kappa}$ and $g_{n,\kappa}$ that have same number of nodes n =0 or 1.

For the PSF computation, all integrals in Eq. (5) were performed accurately with Gauss-Legendre quadrature in 32 points. We calculated up to 49 values of the ra-

dial functions in the Q value energy interval, that were interpolated with spline functions.

We also calculated the PSF for EC process using Eq. (15) but employing essentially the formalism adopted by Ref. [2]. Here we used the electron radial density (and density ratios) as given in Table 2 of [2]. Exchange corrections were taken as unity. Binding energies were also taken from the same reference.

III. RESULTS AND DISCUSSION

We perform PSF computations for the β^+ decay and the EC process with the method described in the previous section, that we call TW (This Work), for a large number of nuclei of experimental interest.

For the β^+ decays we found previous PSF results computed with approximate methods [14, 15], for sixteen nuclei of astrophysical interest. In Table I we display the PSF values for these nuclei calculated with our new method (TW) and, for comparison, the values taken from [14, 15]. Also, we present the PSF values computed by us using the recipe described in Ref. [3]. All calculations were done with the W_0 value indicated in [14]. One can see that the agreement between TW results and the other results are in general under 1%, except the last two (heaviey) nuclei where the differences reach $\sim 3\%$.

In Table II we display our PSF computed with the new method for few heavy nuclei, but for which we did not find previous results. For comparison we computed the same PSF values with the recipe adopted from Ref. [3]. W_0-values were taken from [20] for both sets of calculations. We found a rather good agreement between the two sets of result, with differences within, generally, a few percent. There was one exception, ^{105}Ag, where the difference was large ($\sim$ a factor 10). This is a case where the W_0-value is very small (0.325 MeV), and might make our numerical routine to be inaccurate at such small values. However, this discrepancy may not be so significant, as long as the calculated PSF value is small enough to have little contribution to the corresponding beta decay rates

In Table III we preset our results for EC for the same set of nuclei. The Q-values for positron decay were taken from Ref. [14] for nuclei marked with $\star$. For the rest of nuclei the Q-values were taken from Ref. [20]. Together with the PSF values for EC, the electron densities, g_{K,L_1}, their ratios and the binding energies ϵ for the orbitals $1s_{1/2}$ and $2s_{1/2}$ are also given in Table III. We compare the results performed with the new method (TW) with those calculated using the recipe of Ref. [2]. For these transitions the differences between the two sets of results are significantly larger than for the positron decays, ranging from a few percent to about a mammoth 35%. We attribute these differences in the calculated PSF values mainly due to electron densities, g_K, whose values, calculated with the "old"' and "new"' methods, differ significantly from each other. We also checked the influence of the screening effect on the PSF values. We found that while for the positron decays this effect is very small, for the EC transitions there is some differences between the "'screened"' and "'un-screened" PSF values. Fig. 1 shows this effect on the electron density, g_K and on the final PSF values. For small values of Z the results without screening give PSF values that are 10-15% larger than those listed in Table III. For heavier nuclei, these differences are only up to 2-3%. The screening effect in PSF calculation is more important for light nuclei and lead to a decrease in the PSF values up to 15%. Finally, in Table IV we present PSF values for EC transitions, re-computed with up-dated Q-values taken from Ref. [13]. We propose to use these new computed values of PSF for calculation of β decay rates.

IV. SUMMARY AND CONCLUSION

In summary, we constructed a new code for computing PSF values for positron decays and EC processes. In our approach we get positron free and electron bound w.f. by solving a Dirac equation with a Coulomb-type potential, obtained from a realistic distribution of protons in the daughter nuclei. The FNS and screening effects are addressed as well by our new recipe. Using the same Q-values, we compare our results with previous calculations where electron/positron w.f. were obtained in an approximate way. For positron decays the agreement with older results is quite good, while for EC processes the differences between "new" and "old" PSF values is as big as 35%. We further found that the screening effect is important for EC processes, specially for light nuclei, having an impact up to 10-15% on the calculated PSF values. Finally, using our new method, we re-computed the PSF for all nuclei using up-dated Q-values. We hope, these computed PSF values will prove useful in more accurate estimations of the beta decay rates. We are currently working on the impact of newly computed PSF values on β-decay half-lives and hope to report our findings in near future.

Acknowledgments S. Stoica, M. Mirea would like to acknowledge the support of the ANCSI-UEFISCDI through the project PCE-IDEI-2011-3-0318, Contract no. 58.11.2011.

J.-U. Nabi would like to acknowledge the support of the Higher Education Commission Pakistan through the HEC Project No. 20-3099.

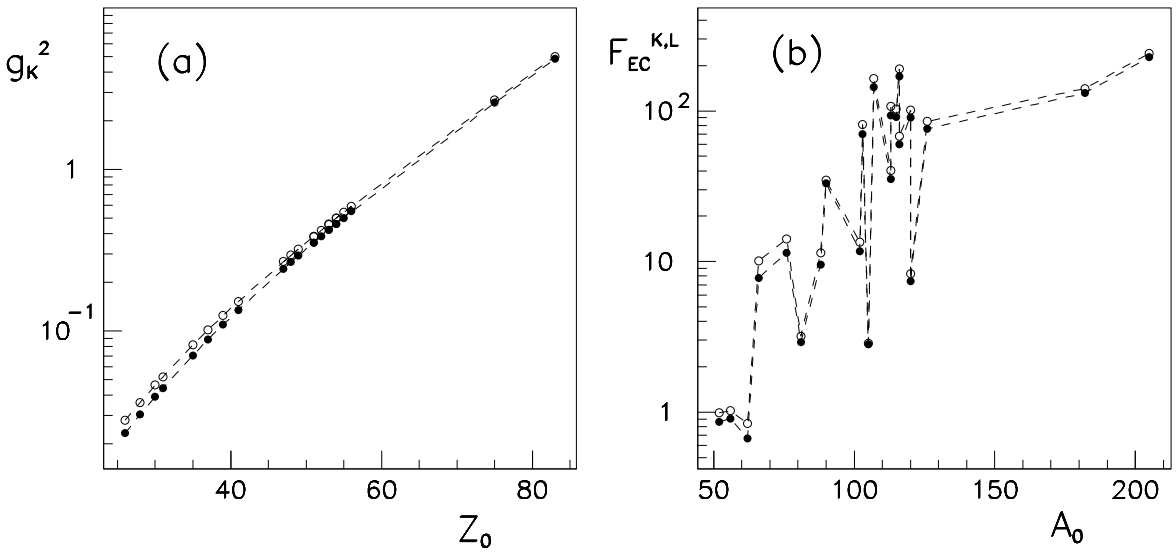

FIG. 1. (a) Electron density on the nuclear surface of the $1s_{1/2}$ state as a function of the atomic number of the parent nucleus. The values calculated with screening are displayed with filled circles and those without screening are plotted with empty symbols. The dashed lines are given to guide the eye. (b) Calculated PSF for EC as a function of the mass number of the parent nucleus. The filled circles display the calculation with screening, while the empty ones the calculation without screening.

[1] H. Behrens, J. Janecke, Numerical Data and Functional Relationships in Sci.Technol., Landolt-Bornstein, New Ser., H.Schopper, Ed.,Springer-Verlag, Berlin, Group 1: Nucl. Phys. Technol., **4**, 1 (1969).

[2] M. J. Martin and P. H. Blichert-Toft, Nucl. Data Tables **A8**, 1 (1970).

[3] N. B. Gove and M. J. Martin, Nucl. Data Tables, **10**, 205, 1971.

[4] M.E.Rose, Phys. Rev. 49, 727 (1936).

[5] R.H.Good, Jr., Phys. Rev. 94, 931 (1954).

[6] M.E.Rose and D.K.Holmes, Phys.Rev. 83, 190 (1951).

[7] M.E.Rose and D.K.Holmes, ORNL-I022 (1957).

[8] R.B.Elton, Nuclear Sizes, Oxford Unlv. Press, London (1961).

[9] W. Buhring, Z. Phys. **187**, 180 (1965).

[10] F. Salvat, R. Mayol, Comp. Phys. Commun. 62, 65 (1991).

[11] F. Salvat, J.M. Fernandez-Varea, W. Williamson Jr, Comp. Phys. Commun. 90, 151 (1995).

[12] S. Esposito, Am. J. Phys. **70**, 852 (2002).

[13] G. Audi, M. Wang, A. H. Wapstra, F. G. Kondev, M. MacCormick, X. Xu and B. Pfeiffer, Chin. Phys. C, **36** 1287 (2012); M. Wang, G. Audi, A. H. Wapstra, F. G. Kondev, M. MacCormick, X. Xu and B. Pfeiffer B, Chin. Phys. C, **36** 1603 (2012).

[14] D. H. Wilkinson and B. E. F. Macefield, Nucl. Phys. **A232**, 58 (1974).

[15] I. S. Towner and J. C. Hardy, Nucl. Phys. A205 (1973) 33.

[16] J. Kotila, F. Iachello, Phys. Rev. C 85, 034316 (2012).

[17] S. Stoica, M. Mirea, Phys. Rev. C **88**, 037303 (2013).

[18] M. Mirea, T. Pahomi, S.Stoica, Rom. Rep. Phys. **67**, 872 (2015).

[19] J.N. Bahcall, Phys. Rev. **132**, 362 (1963).

[20] G. Audi and A. H. Wapstra, Nucl. Phys. A **595**, 409 (1995).

[21] G. Audi, O. Bersillon, J. Blachot and A. H. Wapstra, Nucl. Phys. A **729**, 3-128 (2003).

[22] A. Staudt, E. Bender, K. Muto and H. V.Klapdor-Kleingrothaus, At. Data. Nucl. Data Tables, **44**, 79 (1990)

[23] P. Möller and J. R. Nix, At. Data Nucl. Data Tables, **26**, 165 (1981).

[24] J.-U. Nabi and H. V. Klapdor-Kleingrothaus, At. Data Nucl. Data Tables 71, 149 (1999).

[25] J.B. Mann and J.T. Waber, At. Data **5**, 201 (1973).

[26] T.C. Tucker et al., Phys, Rev. **178**, 998 (1969).

TABLE I. Calculated phase space of β^+-decay (BP) compared with previous calculations. The value of maximum β-decay energy is taken from [14] for pure Fermi transitions. The last two columns show our calculated results.

Nucleus	W_0[14] (MeV)	F_{BP} [15]	F_{BP}[14]	F_{BP}[TW]	F_{BP}[3]
^{10}C	0.8884	2.361	2.361	2.325	2.326
^{14}O	1.8098	43.398	43.378	42.822	42.814
^{18}Ne	2.383	136.83	136.83	135.19	135.08
^{22}Mg	3.109	427.02	426.88	422.19	421.51
^{26}Al	3.211	483.84	483.68	478.3	477.43
^{26}Si	3.817	1036.8	1035.9	1025.51	1023.059
^{30}S	4.439	1990.2	1987.8	1969.24	1963.9
^{34}Cl	4.468	2014.7	2013.4	1993.13	1987.4
^{34}Ar	5.021	3388.3	3383.8	3351.58	3339.85
^{38}K	5.028	3346.9	3344.9	3312.82	3300.54
^{38}Ca	5.620	5515.9	5510.3	5457.95	5449
^{42}Sc	5.409	4533.5	4531.7	4490.19	4462.21
^{42}Ti	5.964	7025.4	7024.1	6934.9	6853.74
^{46}V	6.032	7285.9	7284.2	7186.04	7091.9
^{50}Mn	6.609	10818	10810	10492.76	10262
^{54}Co	7.227	15956	15951	14988.470	14412.5

TABLE II. Calculated phase space of β^+-decay (BP) for heavy nuclei compared with the ones we calculated using recipe of [3].

Nucleus	W_0 [20] (Mev)	$F_{BP}[TW]$	F_{BP} [3]
^{52}Fe	1.3525	8.3403	8.4132
^{56}Ni	1.1109	3.4439	3.5250
^{62}Zn	0.5974	0.2344	0.2438
^{66}Ga	4.153	1125.6442	1132.5483
^{76}Br	3.9409	835.1982	843.3343
^{81}Rb	1.2161	4.3222	6.8878
^{88}Y	2.6006	120.2644	121.8624
^{90}Nb	5.0893	2503.0555	2533.7049
^{102}Cd	1.565	11.2214	11.5267
^{103}In	5.0005	2100.3727	2136.0153
^{105}Ag	0.325	0.0102	0.1127
^{107}Sb	6.837	8528.5047	8931.8197
^{113}Sb	2.8891	168.1487	172.0209
^{113}Te	5.048	2124.1816	2165.2927
^{115}I	4.7029	1517.2376	1549.2409
^{116}I	6.7547	7913.1790	8272.0244
^{116}Xe	3.235	352.3565	361.4082
^{120}Ba	3.98	678.0918	705.0294
^{120}Xe	0.5587	0.1047	0.1108
^{126}Cs	3.7731	542.4653	563.8184
^{182}Re	1.778	16.123	17.206
^{205}Bi	1.6835	12.3984	13.4576

TABLE III. Calculated phase space factors F_{EC} for electron capture (assuming exchange corrections to be equal to 1). The value of maximum β-decay energy is taken from [14] for pure Fermi transitions. The electron densities, their ratios, and the binding energies ϵ are also provided for the orbitals $1s_{1/2}$ and $2s_{1/2}$, including those given in [2]. Binding energies are given in units of keV.

Nucleus	$Q_{\beta+}$ (MeV)	g_K^2 [2]	g_K^2[TW]	$g_{L_1}^2/g_K^2$ [2]	$g_{L_1}^2/g_K^2$[TW]	ϵ_K [2]	ϵ_K [TW]	ϵ_{L_1} [2]	ϵ_{L_1}[TW]	F_{EC}^{K,L_1}[TW]	F_{EC}^{K,L_1} [2]
$^{10}C^{\star}$	1.9104	0.00031	0.00031	0.04930	0.02867	0.18790	0.62660	0.12600	0.01176	0.00703	0.00640
$^{14}O^{\star}$	2.83186	0.00075	0.00065	0.05640	0.04420	0.40160	1.03733	0.02440	0.03251	0.03297	0.03786
$^{18}Ne^{\star}$	3.405	0.00151	0.00118	0.05840	0.05794	0.68540	1.48302	0.03400	0.06659	0.08713	0.11005
$^{22}Mg^{\star}$	4.131	0.00268	0.00199	0.06660	0.06811	1.07210	2.11143	0.06330	0.15721	0.218	0.29060
$^{26}Al^{\star}$	4.2331	0.00344	0.00251	0.06990	0.07265	1.30500	2.40715	0.08940	0.14631	0.27558	0.39270
$^{26}Si^{\star}$	4.839	0.00435	0.00312	0.07290	0.07661	1.55960	2.74689	0.11770	0.18077	0.47240	0.65060
$^{30}S^{\star}$	5.461	0.00664	0.00467	0.07810	0.08342	2.14550	3.49498	0.18930	0.25934	0.90680	1.27140
$^{34}Cl^{\star}$	5.4908	0.00807	0.00563	0.08040	0.08628	2.47200	3.91749	0.22920	0.30899	1.10727	1.56600
$^{34}Ar^{\star}$	6.043	0.00970	0.00675	0.08240	0.08862	2.82240	4.33190	0.27020	0.36199	1.61130	2.28490
$^{38}K^{\star}$	6.05	0.01156	0.00802	0.08440	0.09079	3.20600	4.77984	0.32630	0.41921	1.92311	2.73480
$^{38}Ca^{\star}$	6.642	0.01367	0.00947	0.08620	0.09259	3.60740	5.25087	0.37710	0.48351	2.74237	3.90650
$^{42}Sc^{\star}$	6.4311	0.01600	0.01113	0.08790	0.09430	4.03810	5.73657	0.43780	0.54865	3.02434	4.28930
$^{42}Ti^{\star}$	6.986	0.01870	0.01300	0.08960	0.09579	4.49280	6.25222	0.50040	0.62068	4.17496	5.92320
$^{46}V^{\star}$	7.0543	0.02170	0.01512	0.09100	0.09699	4.96640	6.78377	0.56370	0.69826	4.95575	7.02120
$^{50}Mn^{\star}$	7.6311	0.02870	0.02016	0.09380	0.09920	5.98920	7.92722	0.69460	0.86703	7.74617	10.9103
^{52}Fe	2.374	0.0328	0.0232	0.0950	0.0987	7.1120	8.5130	0.8461	0.958	0.859	1.2033
$^{54}Co^{\star}$	8.2498	0.03730	0.02651	0.09620	0.10077	7.11200	9.14731	0.84610	1.05584	11.91799	16.6144
^{56}Ni	2.136	0.0423	0.0303	0.0974	0.1013	8.3328	9.7882	1.0081	1.158	0.907	1.2580
^{62}Zn	1.626	0.0538	0.0390	0.0995	0.1025	9.6586	11.157	1.1936	1.380	0.675	0.9261
^{66}Ga	5.175	0.0604	0.0410	0.1006	0.1029	10.3671	11.875	1.2977	1.498	7.80	10.613
^{76}Br	4.963	0.0935	0.0704	0.1035	0.1048	13.4737	15.000	1.7820	2.021	11.45	15.162
^{81}Rb	2.23815	0.1149	0.0883	0.1063	0.1080	15.1997	16.690	2.0651	2.263	9.069	11.744
^{88}Y	3.6226	0.1402	0.1091	0.1080	0.1174	17.0384	18.450	2.3725	2.438	9.528	12.114
^{90}Nb	6.111	0.170	0.1344	0.1098	0.1059	18.9856	20.421	2.6977	2.994	33.17	41.975
^{102}Cd	2.587	0.319	0.2663	0.1159	0.1102	26.7112	28.044	4.0180	4.351	11.66	14.019
^{103}In	6.050	0.348	0.2930	0.1168	0.1116	27.9399	29.232	4.2375	4.548	71.05	84.541
^{105}Ag	1.345	0.293	0.2423	0.1150	0.1086	25.5140	26.864	3.8058	4.161	2.816	3.4256
^{107}Sb	7.920	0.413	0.3526	0.1187	0.1096	30.4912	31.726	4.6983	5.095	146.5	172.43
^{113}Sb	3.913	0.413	0.3516	0.1187	0.1096	30.4912	31.726	4.6983	5.095	35.38	41.804
^{113}Te	6.070	0.449	0.3844	0.1196	0.1113	31.8138	33.041	4.9392	5.314	93.70	109.93
^{115}I	5.729	0.488	0.4121	0.1205	0.1124	33.1694	34.345	5.1881	5.542	91.54	106.40
^{116}I	7.780	0.488	0.4215	0.1205	0.1124	33.1694	34.345	5.1881	5.542	169.3	196.75
^{116}Xe	4.450	0.529	0.4609	0.1215	0.1123	34.5644	35.705	5.4528	5.822	60.15	69.410
^{120}Ba	5.00	0.623	0.5496	0.1234	0.1130	37.4406	38.514	5.9888	6.375	90.65	103.51
^{120}Xe	1.617	0.529	0.4599	0.1215	0.1123	34.5644	35.705	5.4528	5.821	7.72	8.9482
^{126}Cs	4.824	0.574	0.501	0.1224	0.112	35.9846	37.111	5.7143	6.128	76.88	88.697
^{182}Re	2.800	2.69	2.593	0.1448	0.128	71.6764	72.491	12.5267	13.26	22.86	24.152
^{205}Bi	2.708	4.88	4.837	0.1561	0.138	90.5259	91.373	16.2370	17.25	228.17	233.83

TABLE IV. Calculated phase space factors F_{EC} for electron capture, with Q-values from [13].

Nucleus	Q_{EC}[13] (MeV)	F_{EC}[TW]	F_{EC}[2]	F_{BP}[TW]	F_{BP}[3]
^{10}C	3.64613	0.07318	2.33265	226.780	226.834
^{14}O	5.14131	0.21794	0.12483	1644.76	1643.41
^{18}Ne	4.44215	0.27831	0.18733	677.970	677.912
^{22}Mg	4.77904	0.61616	0.39020	995.887	995.685
^{26}Al	4.00231	0.62642	0.35240	343.398	343.658
^{26}Si	5.06645	0.51788	0.71694	1339.344	1339.30
^{30}S	6.13834	1.14585	1.61931	3805.276	3803.16
^{34}Cl	5.48869	1.10642	1.57889	1994.797	1995.09
^{34}Ar	6.05858	1.61963	2.31915	3410.133	3409.96
^{38}K	5.91093	1.83565	2.64042	2917.839	2918.62
^{38}Ca	6.73867	2.82284	4.07367	5924.355	5929.26
^{42}Sc	6.42269	3.01643	4.33609	4470.946	4471.87
^{42}Ti	7.01275	4.20702	6.05196	7100.190	7130.06
^{46}V	7.04865	4.94781	7.11022	7175.692	7209.06
^{50}Mn	7.63042	7.74479	11.0705	10516.941	10744.5
^{52}Fe	2.37330	0.8584	1.22082	14942.286	15765.2
^{54}Co	8.24017	11.89015	16.8306	8.354	8.43206
^{56}Ni	2.13175	0.9029	1.27259	3.444	3.49486
^{62}Zn	1.61859	0.6687	0.93259	0.234	0.24131
^{66}Ga	5.17225	7.7902	10.7797	1125.644	1131.60
^{76}Br	4.96024	11.439	15.4388	835.295	841.531
^{81}Rb	2.23696	2.9044	3.84415	4.321	4.41092
^{88}Y	3.62067	9.5180	12.3759	120.264	121.864
^{90}Nb	6.10809	33.141	42.9337	2502.372	2526.00
^{102}Cd	2.58562	11.652	14.4027	11.221	11.5468
^{103}In	6.01928	70.333	15.7203	2099.402	2133.61
^{105}Ag	1.34679	2.8233	3.53114	0.01027	1.12362
^{107}Sb	7.85483	144.059	174.745	8528.505	8918.59
^{113}Sb	3.90909	35.311	42.9919	168.122	172.036
^{113}Te	6.06682	93.601	113.234	2124.182	2162.53
^{115}I	5.72192	91.3148	109.531	1509.977	1547.75
^{116}I	7.77260	168.959	202.635	7930.046	8250.78
^{116}Xe	4.44315	59.963	71.4659	354.467	361.241
^{120}Ba	4.99761	90.562	106.993	685.518	703.098
^{120}Xe	1.57992	7.3638	8.82085	0.105	0.11187
^{126}Cs	4.79256	75.871	90.4835	542.400	555.411
^{182}Re	2.79851	131.273	145.184	16.123	17.2282
^{205}Bi	2.70412	227.499	247.263	12.415	13.4798